

# **Surface treatment of an Al<sub>2</sub>O<sub>3</sub>-based refractory with CO<sub>2</sub> and high power diode lasers for improved mechanical and chemical resistance characteristics**

J. Lawrence\* and L. Li\*\*

\*Manufacturing Engineering Division, School of Mechanical & Production Engineering, Nanyang Technological University (NTU), Nanyang Avenue, Singapore 639798.

\*\*Laser Processing Research Centre, Department of Mechanical, Aerospace and Manufacturing Engineering, University of Manchester Institute of Science and Technology (UMIST), Manchester, M60 1QD, UK.

## Correspondence

Dr. Jonathan Lawrence  
Manufacturing Engineering Division,  
School of Mechanical & Production Engineering,  
Nanyang Technological University (NTU),  
Nanyang Avenue,  
Singapore 639798.

Tel : (+65) 6790 5542

Fax : (+65) 6791 1859

email : [mjlawrence@ntu.edu.sg](mailto:mjlawrence@ntu.edu.sg)

## **Abstract**

Within both normal and corrosive (NaOH and HNO<sub>3</sub>) environmental conditions, the wear rate and wear life characteristics of an Al<sub>2</sub>O<sub>3</sub>-based refractory were greatly enhanced by means of CO<sub>2</sub> and high power diode laser (HPDL) surface treatment. Such improvements are attributed to the fact that after laser treatment, the microstructure of the Al<sub>2</sub>O<sub>3</sub>-based refractory was altered from a porous, randomly ordered structure, to a much more dense and consolidated structure that contained fewer cracks and porosities. What is more, resulting from the different rates of solidification brought about by differences in the wavelengths of the two lasers, dissimilar microstructures were subsequently generated. Indeed, despite the fact that the glaze thickness was less, the wear life of the HPDL treated surface exceeded that of the CO<sub>2</sub> laser treated surface in all the test environments owing to its finer, more densely packed and less cracked microstructure.

*Keywords:* Laser; Refractory; Al<sub>2</sub>O<sub>3</sub>; Surface glazing; Erosion; Corrosion; Wear; Life characteristics

## 1. Introduction

The current and foreseeable global economy demands that material conservation becomes a matter of increasing importance. Erosion and corrosion are significant causes of wastage in many high temperature applications where materials such as refractories are employed. This ultimately necessitates the arduous and costly undertaking of replacing the affected refractory. It is therefore obvious that any means whereby the life of the refractory could be extended would be of great interest to all engineers, for any reduction in the wear of the refractory could bring about significant economic savings. This present work is concerned with establishing and comparing the erosion and corrosion characteristics of a glaze generated on the surface of an  $\text{Al}_2\text{O}_3$ -based refractory by means of a  $\text{CO}_2$  laser and a high power diode laser (HPDL).

On account of their physical and chemical stability at high temperatures, refractory materials find use in application areas such as linings for furnaces and incinerators. As part of their normal operating cycle, the linings must withstand, amongst other things, mechanical wear due to the movement of the contents and chemical attack from heated solids, liquids and/or gasses [1]. In addition, energy requirements demand that the linings provide the optimum amount of heat insulation [2]. On the one hand, porous refractories will act as effective insulators since porosity is inversely proportional to thermal conductivity [3], but on the other, such materials are susceptible to penetration by corrosive reagents during operation. Indeed, it is known that denser refractories degrade less because penetration is hindered by their more closely packed structure [4]. The protection of refractories exposed to aggressive high temperature environments generally depends on the formation of an effective diffusion barrier layer which possesses superior erosion and corrosion properties to the bulk. Existing methods for providing improved erosion and corrosion protection for refractories are based either on tailoring the manufacturing process or using a coating. Typically, tailoring of the manufacturing process involves techniques for densification of the refractory material [2]. As for coatings, established technologies using chemical, mechanical and/or thermal methods are employed to apply surface layers [5, 6]. However, problems such as residual stress generation, low production rates, coating stability, microcracking and porosity are often attendant with these methods [7, 8].

The relatively recent emergence of the technology of laser materials processing offers a viable alternative to the existing methods for improving the erosion and corrosion resistance of refractories. Moreover, many of the disadvantages associated with the existing methods may be eliminated due to the operating characteristics of the laser technology. In particular, the surface treatment of materials with lasers has the major advantage that a large amount of energy can be focused on a small area. This very localised heating means that controllability of the melt depth is possible through the manipulation of the laser operating parameters. Several successful studies have shown the feasibility

of using lasers to improve the surface characteristics of various ceramic and composite materials. The remelting of  $\text{ZrO}_2$ -based protective ceramic layers using a  $\text{CO}_2$  laser [9] was shown to result in a marked decrease in the level of structural defects. Further, the  $\text{CO}_2$  laser remelting of a number of oxide ceramic coatings has been found to effect significant improvements in corrosion resistance [10], whilst the  $\text{CO}_2$  laser remelting of  $\text{Al}_2\text{O}_3$  and  $\text{Al}_2\text{O}_3$ - $\text{TiO}_2$  coatings yielded an increase in hardness and wear resistance [11]. The remelting of  $\text{ZrO}_2$ -based protective ceramic layers plasma sprayed onto a variety of bond coats using continuous wave (CW) and pulsed  $\text{CO}_2$  lasers [12, 13] revealed that the pulsed laser produced less cracking. The laser melting of plasma sprayed ceramic coatings based on  $\text{Al}_2\text{O}_3$ ,  $\text{TiO}_2$  and  $\text{ZrO}_2$  using CW and pulsed  $\text{CO}_2$  lasers [14] revealed that the extent of cracking was a function of the total energy input to the surface and the thermophysical properties of the ceramic coatings. After excimer laser treatment of the surface of  $\text{Al}_2\text{O}_3$ , Cappelli et al. [15] noted changes in the surface chemistry and morphology of the material, whilst Wu et al. [16] found that excimer laser treatment of  $\text{Al}_2\text{O}_3$ -SiC occasioned surface smoothing and an increase in the toughness of the material. The surface glazing of mullite with a HPDL by Schmidt and Li [17] resulted in a glaze that exhibited good adherence to the bulk ceramic but was severely cracked. To date, many studies have been carried out to investigate the laser surface processing of concrete. As part of nuclear plant decommissioning, Li et al. [18-21] conducted research to determine the workability of several laser techniques for sealing/fixing radioactive contamination onto concrete surfaces. Work by Sugimoto et al. [22] focused upon modifying the surface appearance and surface properties of cement based materials using a high power  $\text{CO}_2$  laser. The resultant physical characteristics and mechanical behaviour of the post-process cement based materials was later fully characterised by Wignarajah et al. [23]. Borodina et al. [24] has carried out investigations into the structural changes within the composition of zirconia concrete caused by surface exposure to  $\text{CO}_2$  laser radiation. More detailed and comprehensive studies conducted by Lawrence and Li have investigated the feasibility and characteristics of HPDL generated glazes on the ordinary Portland cement (OPC) surface of concrete [25, 26]. In further work Lawrence and Li studied the generation and carried out a comparison of the glazes generated with both  $\text{CO}_2$  and HPDL's [27, 28]. In contrast, investigations into the laser processing of refractories are few in number. Work by Bradley et al. examined the surface treatment of alumina-based refractories with  $\text{CO}_2$  and HPDLs [29, 30] and a xenon arc lamp [31], whilst Lawrence and Li [32] studied the laser beam interaction characteristics of the  $\text{Al}_2\text{O}_3$ -based refractory considered in this work.

## 2. Experimental procedures

### 2.1 Material details

The material used in the experiments was an  $\text{Al}_2\text{O}_3$ -based refractory containing various impurities. The composition by weight of the refractory is as follows:  $\text{Al}_2\text{O}_3$  (83.5%),  $\text{SiO}_2$  (9%),  $\text{Cr}_2\text{O}_3$  (4.5%),  $\text{P}_2\text{O}_5$  (1.6%),  $\text{Fe}_2\text{O}_3$  (0.4%),  $\text{TiO}_2$  (0.3%),  $\text{MgO}$  (0.3%),  $\text{Na}_2\text{O}$  (0.2%),  $\text{CaO}$  (0.1%) and  $\text{K}_2\text{O}$  (0.1%). The refractory material studied is used commercially as a lining in industrial furnaces and incinerators. The refractory was obtained (from Cleanaway) in the form of blocks (200 x 200 x 100 mm<sup>3</sup>). The as-received blocks typically contained 12% porosity with aggregates of 1 to 3 mm in size being evenly distributed throughout the bricks. Furthermore, small sized cracks and porosities were generally visible on the surfaces of the as-received samples. For the purpose of experimental convenience the as-received refractory blocks were sectioned into small cubes (20 x 20 x 10 mm<sup>3</sup>) with only two-thirds being laser treated. The selected refractory samples were treated with both lasers at room temperature and in normal atmospheric conditions.

### 2.2 Lasers and the processing procedure

The lasers used in this work were a  $\text{CO}_2$  laser (Rofin-Sinar, RS1000) emitting at 10.6  $\mu\text{m}$  with a maximum output power of 1 kW and a HPDL (Diomed, D120) emitting at 810 $\pm$ 20 nm with a maximum output power of 120 W. The  $\text{CO}_2$  laser beam was delivered to the work surface by focusing the beam through a 125 mm focal length KC1 lens to give a stable diverging beam. The HPDL beam was delivered to the work area by means of a 4 m long, 1 mm core diameter optical fibre, the end of which was connected to a 2:1 focusing lens assembly. Both lasers were operated in the continuous wave (CW) mode and produced a multi-mode beam. The defocused laser beams were fired across the surface of the samples (the as-received  $\text{Al}_2\text{O}_3$ -based refractory) by traversing the samples beneath the beams using the x- and y-axis of CNC gantry tables. In both instances the laser optics were protected by means of a coaxially blown  $\text{O}_2$  shield gas jet at a rate of 10 l/min. In order to study accurately the differing effects of the two lasers, the power density of each was set at 2 kW/cm<sup>2</sup>, whilst the traverse speed was fixed at 120 mm/min. Further characterisation of the laser generated glazes was achieved by using optical microscopy, scanning electron microscopy (SEM), energy disperse X-ray analysis (EDX) and X-ray diffraction (XRD) techniques.

### 2.3 Wear testing procedure

To determine the wear resistance characteristics of the  $\text{CO}_2$  and HPDL generated glazes on the surface of the  $\text{Al}_2\text{O}_3$ -based refractory, and also those of the as-received surface, wear tests were conducted in accordance with Fig. 1. All the samples, as-received and laser treated, were weighed and then clamped individually in the vice of a common shaping machine. A steel abrader was

attached to the floating head of the shaping machine and moved cyclically back and forth across the as-received and laser glazed  $\text{Al}_2\text{O}_3$ -based refractory surfaces. The total distance moved in one cycle was 6 mm while the traverse speed was 180 mm/min. By applying weights to the floating head a frictional force of 60 N was generated. The samples were subjected to the frictional force for 8 h, being removed from the machine and weighed at 2 h intervals.

### 3. Results

#### 3.1 Wear characteristics in normal environmental conditions

In the main, the resistance of any material to erosion (wear) is related primarily to the hardness of the material in comparison with that of other materials with which it comes into contact [33]. However, wear resistance is not directly proportional to hardness, nor does it always increase with hardness [34]. Fig. 2 shows the relationship between weight loss and the friction time for the  $\text{CO}_2$  and the HPDL generated glazes, as well as those for the as-received  $\text{Al}_2\text{O}_3$ -based refractory surfaces. As is evident from Fig. 2, the wear resistance of both the  $\text{CO}_2$  and HPDL generated glazes displayed a significant increase in wear resistance over the as-received surface, with the weight loss being approximately 1.5 times lower after 4 h, and 3 times lower after 8 h.

#### 3.2 Wear characteristics in corrosive environments

To obtain an idea of how the corrosion resistance of the  $\text{CO}_2$  and HPDL generated glazes compared with that of the as-received surface, corrosion resistance tests based upon BS 6431 [35] were conducted using nitric acid ( $\text{HNO}_3$ ) and sodium hydroxide ( $\text{NaOH}$ ). The experiments were carried out by dropping small amounts of the corrosive agents, in the concentration ratios of 80%, 60%, 40%, 20% and 10%, on to the as-received and laser glazed surfaces of the  $\text{Al}_2\text{O}_3$ -based refractory at hourly intervals for 4 h. Thereafter the samples were examined optically and subjected to the mechanical wear test described earlier and shown in Fig. 1. It is worth mentioning that high concentrations of the corrosive agents were used to simply accelerate the tests.

Both reagents in the concentrations 80% and 60% were seen to attack immediately the as-received surface of the  $\text{Al}_2\text{O}_3$ -based refractory with a similar degree of severity. In marked contrast, both laser glazed surfaces displayed no discernible change in either morphology or microstructure. The variation in wear resistance of the as-received surface of the  $\text{Al}_2\text{O}_3$ -based refractory when exposed to the reagents with an 80% concentration is shown in Fig. 3. As is clearly apparent from Fig. 3, the wear resistance of the refractory is significantly affected when exposed to a corrosive environment. As one can see, the weight loss of the as-received sample was approximately 4 times higher than either laser glaze after 4 h and approximately 10 times higher after 8 h for the  $\text{HNO}_3$ . In the case of

the NaOH, the weight loss was slightly less after both 4 and 8 h. Conversely, as can be seen in Table 1, only a marginal increase in the wear rate was observed for both laser treated surfaces.

## 4. Discussion

### *4.1. Comparative analysis of the as-received surface and the CO<sub>2</sub> and high power diode laser glazed surfaces*

It is clear from the results of the wear tests that the wear resistance characteristics of the Al<sub>2</sub>O<sub>3</sub>-based refractory are greatly improved after surface glazing with either the CO<sub>2</sub> or the HPDL. This improvement in wear rate was especially apparent when the tests were conducted in corrosive environments. The marked difference in wear rate between the laser glazed and as-received Al<sub>2</sub>O<sub>3</sub>-based refractory, in both normal and corrosive environments, can be attributed completely to the difference in structure of the surfaces. In the as-received condition, the surface of the Al<sub>2</sub>O<sub>3</sub>-based refractory is comprised of a porous, randomly ordered structure, whereas the laser glazed surfaces consist of a much more dense and consolidated structure that contains fewer cracks and porosities. Coupled with this is the fact that the laser generated glazes are considerably harder than the as-received surface of the Al<sub>2</sub>O<sub>3</sub>-based refractory, a respective value of around 6 compared to 2 on the Mohs scale. These two major alterations in the nature of the surface of the Al<sub>2</sub>O<sub>3</sub>-based refractory will subsequently provide the laser generated glazes better wear resistance over an as-received surface. In addition to the improvements in the wear resistance of the Al<sub>2</sub>O<sub>3</sub>-based refractory realised after laser surface treatment, a marked difference in the corrosion resistance of the material was observed after laser treatment also. Since the structure of the laser generated glazes is much more dense and consolidated with fewer porosities, the glaze will naturally possess a greater resistance to corrosive reagents than the porous structure of the as received surface of the Al<sub>2</sub>O<sub>3</sub>-based refractory.

### *4.2. Comparative analysis of the CO<sub>2</sub> and high power diode laser glazed surfaces*

As is evident from both Fig. 2 and Fig. 3, there is a distinct difference in the performance of the CO<sub>2</sub> laser generated glaze and the one resulting from HPDL interaction. Such differences in performance can be accounted for by the differing microstructural characteristics of the two glazes. Whereas the microstructure produced in the HPDL generated glazes consisted of fine needle-shape grains in a multi-directional lattice (see Fig. 4(b)), that of the CO<sub>2</sub> laser generated glazes took the form of a regular distributed coarse columnar structure (see Fig. 4(a)). Naturally the coarser microstructure of the glaze resulting after CO<sub>2</sub> laser treatment will have an adverse effect on the erosion and corrosion resistance of the Al<sub>2</sub>O<sub>3</sub>-based refractory. In addition, as one can see from the cross-sectional analysis of both of the laser generated glazes shown in Fig. 5, considerably more cracks are visible in the

glaze produced after CO<sub>2</sub> laser interaction than that generated with the HPDL. Also, it is worth remarking that many of the cracks in the CO<sub>2</sub> laser generated glaze extend from the surface through the entire cross-section of the glaze and beyond the glaze/substrate interface.

The principal reason behind these microstructural differences, and the resulting variations in the erosion and corrosion performance of the laser generated glazes, is the differing rates of solidification ensuing from interaction of the Al<sub>2</sub>O<sub>3</sub>-based refractory surface with the two lasers. Because the wavelengths of the two lasers are very different (10.6 μm for the CO<sub>2</sub> and around 810 nm for the HPDL), then it follows that the beam absorption characteristics will be different. Indeed, Lawrence and Li [32] found that the length to which the beams of the CO<sub>2</sub> and the HPDL were absorbed by the Al<sub>2</sub>O<sub>3</sub>-based refractory were around 345 μm and 198 μm respectively. Based on these figures it is reasonable to assume that since the CO<sub>2</sub> laser beam is absorbed to a greater depth, then the melt depth will be more and the resulting meltpool will be larger and will therefore cool at a slower rate than that of the HPDL generated meltpool. Such a observation was made during similar investigations on ordinary Portland cement (OPC) carried out by Lawrence and Li [36, 37]. If one considers the theories of constitutional supercooling and morphological stability [38-41], which are illustrated schematically in Fig. 6, then it is apparent that the temperature gradient and the solidification rate of a meltpool govern the resulting microstructure of the solidified material. So, increasing the gradient-rate ( $G/R$ ) ratio causes a progressive change in the solidification characteristics, ranging from fully dendritic to cellular-dendritic to cellular and finally to planer front growth. On the other hand, increasing the cooling rate ( $T=G.R$ ) gives rise to shorter diffusion paths and finer structures. More succinctly,  $G/R$  controls the character of the resultant microstructure, whereas the product,  $G.R$  (cooling rate,  $T$ ) determines the scale of the microstructure. Clearly the faster rate of cooling experienced by the surface of the Al<sub>2</sub>O<sub>3</sub>-based refractory after HPDL interaction effected the observed finer microstructure, whilst the slower cooling rate of the Al<sub>2</sub>O<sub>3</sub>-based refractory after CO<sub>2</sub> laser treatment was responsible for the more coarse microstructure.

Owing to its larger size, the peak temperature of the meltpool resulting from interaction of the CO<sub>2</sub> laser with the surface of the Al<sub>2</sub>O<sub>3</sub>-based refractory will be higher than that present in the HPDL generated meltpool. This higher temperature will consequently produce higher thermal stresses. The thermal stress,  $\sigma$ , induced by a thermal gradient can be calculated using the Kingery equation:

$$\sigma = \frac{E\alpha\Delta T}{1 - \nu} \quad (1)$$

where,  $E$  is Young's modulus,  $\alpha$  is the coefficient of thermal expansion and  $\nu$  is Poisson's ratio.  $\Delta T$  is the difference between the critical temperature (below which stresses can no longer be relieved) and ambient temperature. So, as one can see from (1), the higher value of  $\Delta T$  experienced by the CO<sub>2</sub>



laser generated meltpool will inherently have resulted in an increase in  $\sigma$ . Moreover, the obvious cracking that has taken place in the CO<sub>2</sub> laser generated glaze indicates that the induced level of  $\sigma$  was in excess of the fracture strength of the Al<sub>2</sub>O<sub>3</sub>-based refractory. By the same token, the absence of any discernible signs of cracking in the HPDL generated glaze suggests that the value of  $\Delta T$  experienced in the meltpool was sufficiently low enough not to raise  $\sigma$  above the fracture strength of the Al<sub>2</sub>O<sub>3</sub>-based refractory. However, this assertion for the increased occurrence of cracks in the CO<sub>2</sub> laser generated glaze is in contradiction to the theory that a high cooling rate inherently induces thermal stresses which in turn can lead to crack development in order to relieve the generated thermal stresses.

#### *4.3. Life characteristics of the as-received surface and the CO<sub>2</sub> and high power diode laser glazed surfaces*

The all-round superior erosion and corrosion attributes of the laser generated glazes over the as-received Al<sub>2</sub>O<sub>3</sub>-based refractory surface implies that the life characteristics of the laser glazes may also surpass those of the as-received Al<sub>2</sub>O<sub>3</sub>-based refractory. But in any analysis of the wear life of the materials, the in-situ relative thickness of the laser generated glazes and the as-received Al<sub>2</sub>O<sub>3</sub>-based refractory must be considered in order to give a true interpretation of the actual life characteristics. This is particularly true when considering the wear resistance (with and without exposure to corrosive chemical agents). Accordingly the increase in wear life can be given by

$$\text{Increase in wear life} = \frac{\text{Laser glaze wear life}}{\text{Untreated OPC wear life}} \quad (2)$$

$$\text{where,} \quad \text{Wear life} = \frac{\text{Density (mg/cm}^3\text{)} \cdot \text{Thickness (cm)}}{\text{Wear rate (mg/cm}^2\text{/h}^1\text{)}} \quad (2a)$$

Table 1 summarises the wear rate details and the nominal life increase of the laser generated glazes over the as-received Al<sub>2</sub>O<sub>3</sub>-based refractory. As is clearly evident from Table 1, both laser treated surfaces brought about an increase in the wear life of the Al<sub>2</sub>O<sub>3</sub>-based refractory, regardless of the environment. More specifically, it can be seen that the increase in wear life of the laser generated glazes over the as-received Al<sub>2</sub>O<sub>3</sub>-based refractory surfaces varied markedly depending on the working environment, naturally becoming more pronounced in the corrosive conditions. Furthermore, it is interesting to see that, despite the fact that the glaze thickness was less, the wear life of the HPDL treated surface exceeded that of the CO<sub>2</sub> laser treated surface in all the test environments. From this finding it appears that the finer, more densely packed and less cracked microstructure of

the HPDL generated glaze played a significant role in protecting the bulk of the  $\text{Al}_2\text{O}_3$ -based refractory.

#### 4. Conclusions

Laser treatment of the surface of an  $\text{Al}_2\text{O}_3$ -based refractory with  $\text{CO}_2$  and HPDL radiation was seen to enhance the erosion and corrosion characteristics of the material. Moreover, laser surface treatment was found to effect an increase in the wear life of the  $\text{Al}_2\text{O}_3$ -based refractory in both normal and corrosive ( $\text{NaOH}$  and  $\text{HNO}_3$ ) environmental conditions. Under normal conditions the wear rate of the as-received  $\text{Al}_2\text{O}_3$ -based refractory surface was  $7.13 \text{ mg/cm}^2/\text{h}^1$ , increasing greatly to  $51.25 \text{ mg/cm}^2/\text{h}^1$  and  $78.75 \text{ mg/cm}^2/\text{h}^1$  when exposed to  $\text{NaOH}$  and  $\text{HNO}_3$  respectively. In contrast, only very minor increases in the wear rate were experienced by both laser treated surfaces when tested in the corrosive environments. Life assessment testing revealed that the  $\text{CO}_2$  laser generated glaze had an increase in wear life of 1.13 to 11.79 times over the as-received surface of the  $\text{Al}_2\text{O}_3$ -based refractory depending upon the environment. Likewise the HPDL generated glaze increased the wear life of the  $\text{Al}_2\text{O}_3$ -based refractory by 1.27 to 13.44 times depending upon the environment. The generation of surfaces with improved morphology and microstructure which are more resistant to wear in normal and corrosive environments is cited as the reason for the observed improvements in the wear rate and wear life of the  $\text{Al}_2\text{O}_3$ -based refractory after surface treatment with both lasers. More specifically, the improvements can be attributed to the fact that after laser treatment, the microstructure of the  $\text{Al}_2\text{O}_3$ -based refractory was altered from a porous, randomly ordered structure, to a much more dense and consolidated structure that contained fewer cracks and porosities. What is more, resulting from the different rates of solidification brought about by differences in the wavelengths of the two lasers, dissimilar microstructures were subsequently generated. Indeed, despite the fact that the glaze thickness was less, the wear life of the HPDL treated surface exceeded that of the  $\text{CO}_2$  laser treated surface in all the test environments owing to its finer, more densely packed and less cracked microstructure. It is believed that the economic and material benefits to be gained from the deployment of the laser-based technique for generating such an effective and efficient coating on the surface of the  $\text{Al}_2\text{O}_3$ -based refractory could be significant.

## References

1. W.R. Niessen, Combustion and incineration processes, Dekker, New York (1978).
2. J.D. Gilchrest, Fuels, furnaces and refractories, Pergamon, London (1977).
3. K. Shaw, Refractories and their uses, Applied Science Publishers, London (1972).
4. S. Dellaire, R. Angers, J. Can. Ceram. Soc. 51 (1982) 29-37.
5. J. Pou, P. Gonzalez, E. Garcia, D. Fernandez, J. Serra, B. Leon, S.R.J. Saunders, M. Perez-Amor, Appl. Surf. Sci. 79/80 (1994) 338-343.
6. P. Lambert, B. Marple, B. Arsenault, Proc. Int. Symp. on Developments and Application of Ceramics and New Metal Alloys, Toronto, Canada, (1993) 515-525 (Canadian Institute of Mining, Toronto).
7. Y.G. Gogotsi, V.A. Lavrenko, Corrosion of high performance ceramics, Springer, Berlin (1992).
8. W. Weitoa, R. Streiff, W. Maocai, Mater. Sci. Eng. A 121 (1989) 499-507.
9. Adamski, R. McPherson, Proc. 11<sup>th</sup> Int. Thermal Spraying Conf. New York, USA, (1986) 555-564 (ASME, New York).
10. K. Kobylanska-Szkaradek, Lasers in Eng. 9 (1999) 127-138.
11. Y.Z. Yang, Y.L. Zhu, Z.Y. Liu, Y.Z. Chuang, Mater. Sci. Eng. A, 291 (2000) 168-172.
12. B.L. Mordike, R. Sivakumar, Proc. ECLAT '86, Boston, USA (1986) 373-381 (SPIE, Bellingham).
13. H.L. Tsai, P.C. Tsai, J. Mater. Eng. Performance, 7 (1998) 258-264.
14. R. Sivakumar, B.L. Mordike, J. Surf. Eng. 4 (1998) 127-140.
15. E. Capelli, S. Orlando, D. Sciti, M. Montozzi, L. Pandolfi, Appl. Surf. Sci. 154 (2000) 682-688.
16. Y.N. Wu, Z.C. Feng, J. Liang, J. Mater. Sci. Tech. 16 (2000) 401-404.
17. M.J.J. Schmidt, L. Li, Appl. Surf. Sci. 168 (2000) 9-12.
18. L. Li, P.J. Modern, W.M. Steen, Proc. LAMP '92, Nagaoka, Japan, (1992) 843-848 (High Temperature Society of Japan, Osaka).
19. L. Li, W.M. Steen, P.J. Modern, Proc. ISLOE '93, Singapore, (1994) 25-30 National University of Singapore, Singapore).
20. L. Li, W.M. Steen, P.J. Modern, J.T. Spencer, Proc. RECOD '94, London, UK, (1994) 24-28 (SPIE, Bellingham).

21. L. Li, W.M. Steen, P.J. Modern, J.T. Spencer, Proceedings of EUROPTO '94: Laser Materials Processing and Machining, Frankfurt, Germany, (1994) 84-95 (SPIE, Bellingham).
22. K. Sugimoto, S. Wignarajah, K. Nagai, S. Yasu, Proc. ICALEO '90, Boston, USA, (1991) Vol. 71, 302-312 (Laser Institute of America, Orlando).
23. S. Wignarajah, K. Sugimoto, K. Nagai, Proc. ICALEO '92: Laser Materials Processing, Orlando, USA, (1993) Vol. 75, 383-393 (Laser Institute of America, Orlando).
24. T.I. Borodina, G.E. Valyano, N.I. Ibragimov, E.P. Pakhomov, A.I. Romanov, L.G. Smirnova, P.K. Khabibulaev, J. Phys. Chem. Mater. Treatment, 25 (1995) 541-546.
25. J. Lawrence, L. Li, Optics Laser Tech. 31 (2000) 583-591.
26. J. Lawrence, L. Li, J. Laser Apps. 71 (2000) 1-8.
27. J. Lawrence, L. Li, Mater. Sci. Eng. A, 284 (2000) 93-102.
28. J. Lawrence, L. Li, Mater. Sci. Eng. A, 287 (2000) 25-29.
29. L. Bradley, L. Li, F.H. Stott, Appl. Surf. Sci. 138/139 (1999) 233-239.
30. L. Bradley, L. Li, F.H. Stott, Mater. Sci. Eng. A, 278 (2000) 204-212.
31. L. Bradley, L. Li, F.H. Stott, Appl. Surf. Sci. 154/155 (2000) 675-681.
32. J. Lawrence, L. Li, Appl. Surf. Sci. 168 (2001) 71-74.
33. H. Dickson, Glass: A Handbook for Students and Technicians, Hutchinsons Scientific and Technical Publications, London, 1951.
34. B. Petitbon, L. Boquet, D. Delsart, Laser surface sealing and strengthening of zirconia coatings, Surf. & Coat. Tech. 49 1991 57-61.
35. BS 6431: Part 19: 1984, Ceramic Wall and Floor Tiles: Method for Determination of Chemical Resistance. Glazed Tiles.
36. J. Lawrence, L. Li, Optics Laser Tech. 32 (2000) 11-14.
37. J. Lawrence, E.P. Johnston, L. Li, J. Phys. D. 33 (2000), 745-747.
38. G.A. Chadwick, "Constitutional supercooling and microsegregation", in Fractional solidification (Eds. M. Zief and W.R. Wilcox), Academic Press, New York (1967) pp. 120-128.
39. O. Esquivel, J. Mazumder, M. Bass, S.M. Copely, "Microstructural formation according to the theory of constitutional supercooling" in Rapid solidification processing, principles and technologies II (Eds. R. Mehrabian, B.H. Kear and M. Cohen), Claitors Publishing, Baton Rouge (1980), pp. 150-173.

40. R. Mehrabian, Int. Metals Rev. 27 (1982) 185-209.
41. R.L. Ashbrook, Rapid solidification technology: Source book, ASM International, Metals Park (1983).

## List of Figures

Fig. 1. Schematic illustration of the experimental set-up for the wear tests.

Fig. 2. Relationship between weight loss and friction time for the as-received and laser treated  $\text{Al}_2\text{O}_3$ -based refractory.

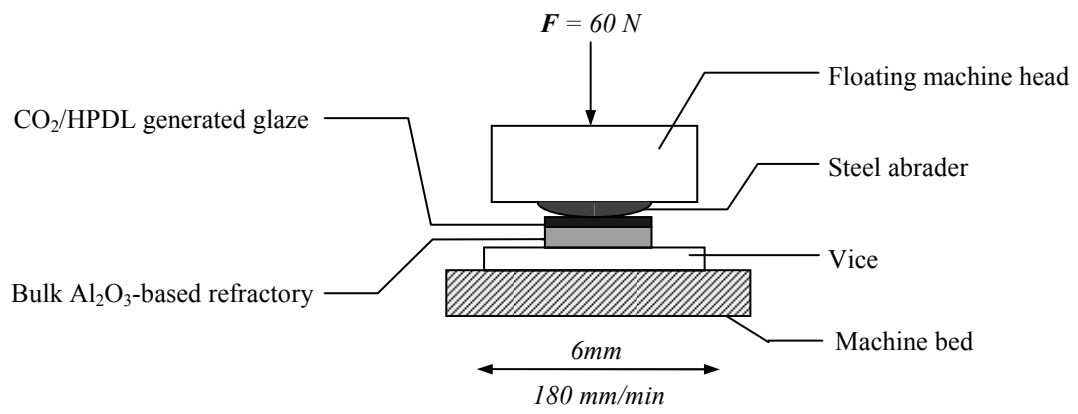
Fig. 3. Relationship between weight loss and friction time for the as-received  $\text{Al}_2\text{O}_3$ -based refractory with different reagent types at the maximum concentration (80%).

Fig. 4. Typical high magnification SEM plan views of (a) the  $\text{CO}_2$  and (b) the HPDL generated glaze on  $\text{Al}_2\text{O}_3$ -based refractory surface.

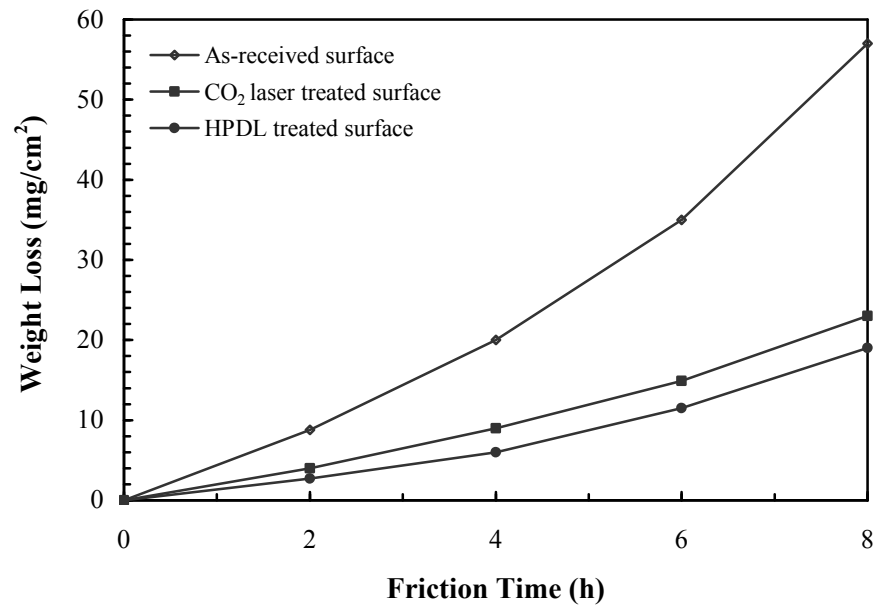
Fig. 5. Typical low magnification SEM cross-sectional views of (a) the  $\text{CO}_2$  and (b) the HPDL generated glaze on  $\text{Al}_2\text{O}_3$ -based refractory surface.

Fig. 6. Dependence of solidification morphology on temperature gradient (G) and solidification rate (R) [39].

**Fig. 1**



**Fig. 2**





**Fig. 3**

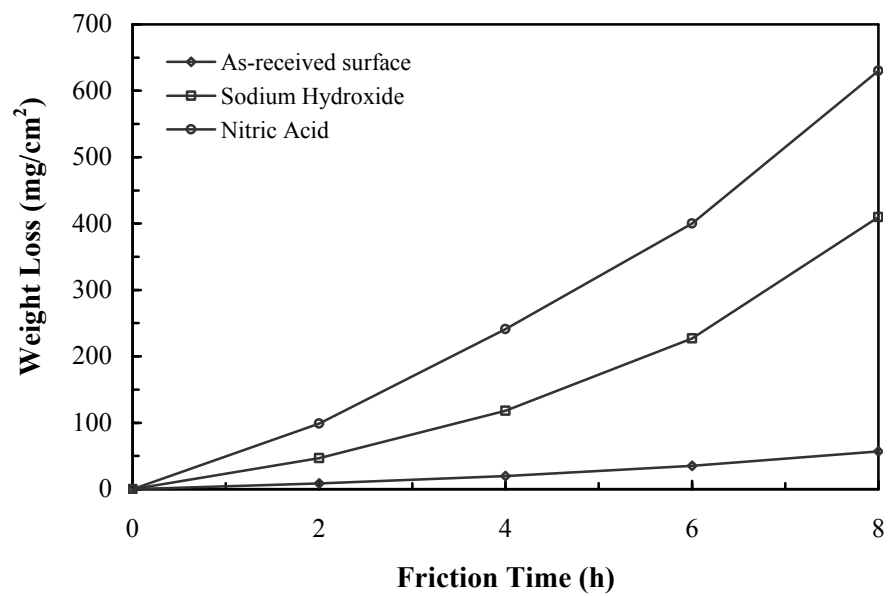
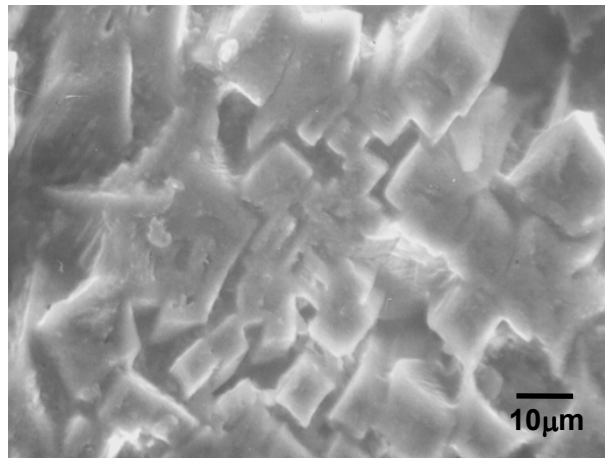
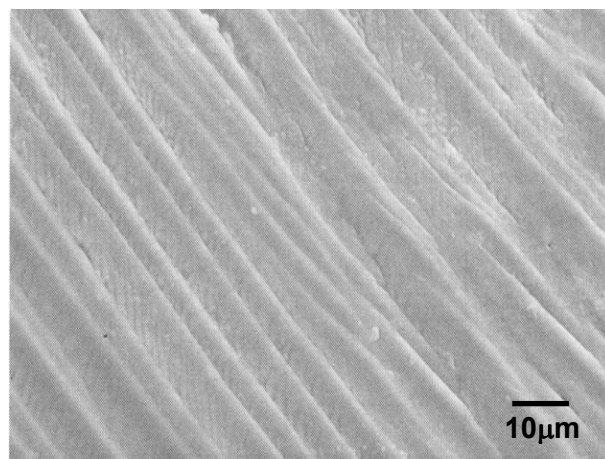


**Fig. 4**

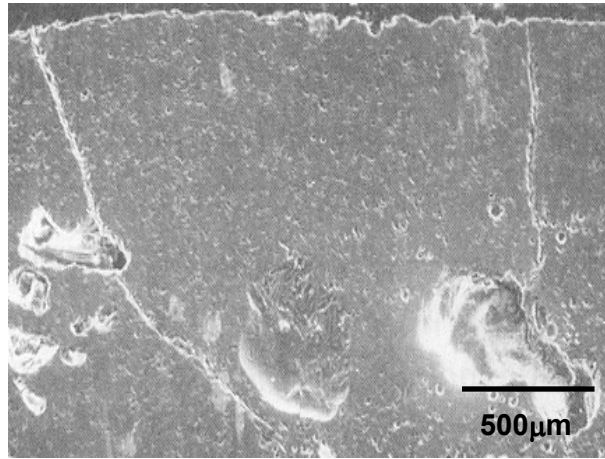


(a)

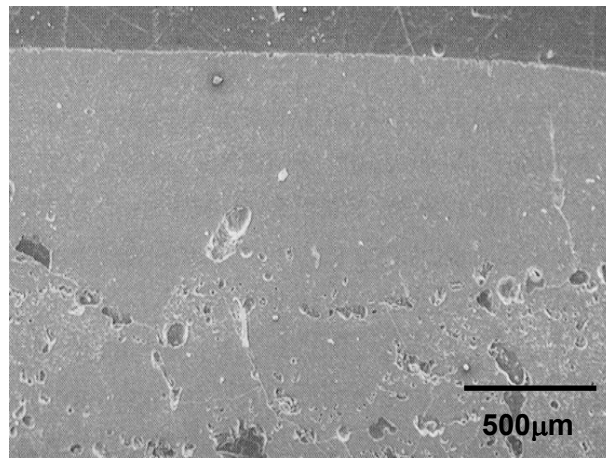


(b)

**Fig. 5**

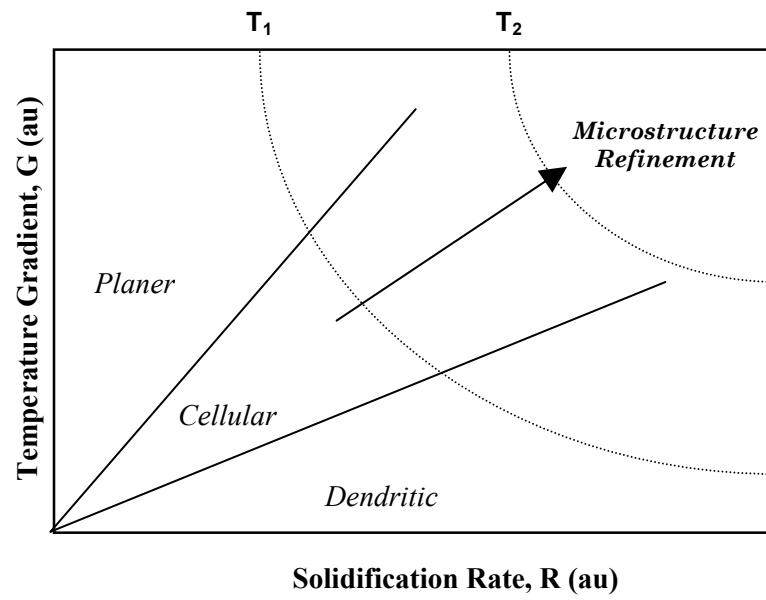


**(a)**



**(b)**

**Fig. 6**



## List of tables

Table 1. Wear rate details and the nominal life increase of the CO<sub>2</sub> and HPDL generated glazes over the as-received Al<sub>2</sub>O<sub>3</sub>-based refractory in normal and corrosive environments.

**Table 1.**

	Density	Thickness	<u>Wear Rate (mg/cm<sup>2</sup>/h<sup>1</sup>)</u>		
			Unexposed	NaOH	HNO <sub>3</sub>
As-received surface	2450 (kg/m <sup>3</sup> )	1.75 (mm)	7.13	51.25	78.75
CO <sub>2</sub> laser treated surface	2600 (kg/m <sup>3</sup> )	0.75 (mm)	2.88	2.95	3.04
<b>Increase in Wear Life</b>	~	~	<b>1.13</b>	<b>7.90</b>	<b>11.79</b>
As-received surface	2450 (kg/m <sup>3</sup> )	1.75 (mm)	7.13	51.25	78.75
HPDL treated surface	2600 (kg/m <sup>3</sup> )	0.70 (mm)	2.38	2.43	2.49
<b>Increase in Wear Life</b>	~	~	<b>1.27</b>	<b>8.95</b>	<b>13.44</b>